Naunyn-Schmiedeberg's Archives of Pharmacology (2022) 395:459–470
https://doi.org/10.1007/s00210-022-02213-7

ORIGINAL ARTICLE

Inhibitory effects on L- and N-type calcium channels by a novel $Ca_V\beta_1$ variant identified in a patient with autism spectrum disorder

Patrick Despang[1] · Sarah Salamon[1] · Alexandra Breitenkamp[1] · Elza Kuzmenkina[1] · Jan Matthes[1]

Received: 16 July 2021 / Accepted: 25 January 2022 / Published online: 5 February 2022

Abstract

Voltage-gated calcium channel (VGCC) subunits have been genetically associated with autism spectrum disorders (ASD). The properties of the pore-forming VGCC subunit are modulated by auxiliary β-subunits, which exist in four isoforms ($Ca_V\beta_{1\text{-}4}$). Our previous findings suggested that activation of L-type VGCCs is a common feature of $Ca_V\beta_2$ subunit mutations found in ASD patients. In the current study, we functionally characterized a novel $Ca_V\beta_{1b}$ variant (p.R296C) identified in an ASD patient. We used whole-cell and single-channel patch clamp to study the effect of $Ca_V\beta_{1b\_R296C}$ on the function of L- and N-type VGCCs. Furthermore, we used co-immunoprecipitation followed by Western blot to evaluate the interaction of the $Ca_V\beta_{1b}$-subunits with the RGK-protein Gem. Our data obtained at both, whole-cell and single-channel levels, show that compared to a wild-type $Ca_V\beta_{1b}$, the $Ca_V\beta_{1b\_R296C}$ variant inhibits L- and N-type VGCCs. Interaction with and modulation by the RGK-protein Gem seems to be intact. Our findings indicate functional effects of the $Ca_V\beta_{1b\_R296C}$ variant differing from that attributed to $Ca_V\beta_2$ variants found in ASD patients. Further studies have to detail the effects on different VGCC subtypes and on VGCC expression.

Keywords Calcium channels · Patch clamp technique · CACNB1 protein · Autism spectrum disorder

Introduction

Autism spectrum disorder (ASD) is a complex neuro-developmental disorder and affects about 1% of the population worldwide (Won et al. 2013). Even though ASD is mainly seen as a genetic disease, the exact etiology is only known in about 20% of the cases, mostly for monogenetic forms of ASD like Timothy syndrome (Splawski et al. 2004; Miles 2011). In ASD, the wide range of genetic findings points to various signaling pathways involved in the manifestation of this disorder (O'Roak et al. 2011; Ebert and Greenberg 2013). A gene pathway analysis with over 2600 patients recognized the "calcium signaling pathway" among the top three pathways involved in ASD (Skafidas et al. 2014). Since the discovery that a single point mutation in the α1-subunit of L-type calcium channels ($Ca_V1.2$) causes Timothy syndrome, many other genes encoding voltage-gated calcium channel (VGCC) subunits have been associated with ASD like the genes *CACNA1B-F* encoding pore-forming subunits, *CACNB1* and *CACNB2* encoding auxiliary β-subunits and, *CACNA2D3* and *CACNA2D4* for auxiliary α_2-δ-subunits (for a comprehensive overview, see Breitenkamp et al. 2015).

Voltage-gated calcium channels (VGCC) are heteromultimeric protein complexes whose composition of pore-forming and auxiliary subunits determines their biophysical properties. High-voltage activated VGCCs are heteromers composed of up to four subunits ($Ca_V\alpha1$, $Ca_V\beta$, $Ca_V\alpha_2$-δ, $Ca_V\gamma$) (Buraei and Yang 2010; Campiglio and Flucher 2015). The subunit of particular importance for the regulation of channel function is the $Ca_V\beta$-subunit, with four different isoforms ($Ca_V\beta_{1\text{-}4}$) involved in the regulation of voltage dependence, channel activity, current kinetics, and also the membrane targeting of functional channels (Meir et al. 2000; Dolphin 2012). Structurally, $Ca_V\beta$-subunits consist of five domains: a variable N-terminus, a conserved Src homology 3 domain (SH3), a conserved but alternatively spliced HOOK domain, a guanylate kinase domain (GK), and a variable C-terminus (Buraei and Yang 2010). With the exception of some rare splice variants, all $Ca_V\beta$-subunits have the same functional structure and show a significant

✉ Jan Matthes
jan.matthes@uni-koeln.de

[1] Center of Pharmacology, Institute II, University of Cologne, Gleueler Strasse 24, 50931 Köln, Cologne, Germany

scale of homology and conservation indicating their functional importance (Hibino et al. 2003; Hofmann et al. 2014).

In a previous study, we found three rare missense mutations in highly conserved regions within the susceptibility gene *CACNB2* in ASD-affected patients, all of them within the HOOK-domain (Breitenkamp et al. 2014). In whole-cell recordings, two of the resulting $Ca_V\beta_2$ mutants (p.G167S, p.S197F) led to a slowed and the third (p.F240L) to an accelerated current inactivation. In a detailed subsequent study, we could show that these mutations and an N-terminal mutation at position 2 (p.V2D) led to a significantly higher single-channel activity compared to channels containing a wild-type (WT) $Ca_V\beta_2$ (Despang et al. 2020). Mutated and WT $Ca_V\beta_2$ subunits interacted with the inhibitory RGK-protein Gem but differed in the extent and characteristics of being modulated by Gem. More recently, we described a homozygous N-terminal $Ca_V\beta_2$ mutant at position 70 (p.R70C) that also showed an increased activity in terms of a reduced inactivation of L-type calcium currents at the whole-cell level (Graziano et al. 2021).

We report here the identification and first electrophysiological characterization of $Ca_V\beta_{1b\_R296C}$, a novel variant of the β_1-isoform of VGCC subunits found in an ASD patient. Different genetic studies suggested that similar to $Ca_V\beta_2$, $Ca_V\beta_1$ may contribute to ASD. A strong evidence of linkage was found for the chromosomal region 17q11-21 that contains *CACNB1*, the gene encoding $Ca_V\beta_1$ (Cantor et al. 2005). In a meta-analysis combining affected sib pairs of five genome-wide linkage scans for ASD, no significant chromosomal region for ASD was found (Trikalinos et al. 2006). However, the authors found two chromosomal regions with a suggestive significance, namely, 17p11.2–q12 and 10p12– q11.1, which comprise the genes encoding $Ca_V\beta_1$ and $Ca_V\beta_2$, respectively.

Given our previous studies indicating Ca^{2+}-current enhancement as a common feature of $Ca_V\beta_2$ variants found in ASD patients, we characterized the electrophysiological properties of the new $Ca_V\beta_1$ variant introduced here. Since the different $Ca_V\beta_2$ variants have shown a kind of "electrophysiological" fingerprint including differential interaction with the RGK-protein Gem, we analyzed $Ca_V\beta_1$-Gem interaction, too. We chose $Ca_V1.2$ as a pore-forming subunit for several reasons: (1) $Ca_V1.2$ is expressed in neuronal tissue and has been associated with several neuropsychiatric diseases (Catterall et al. 2021). (2) A mutant $Ca_V1.2$ protein characterized by impaired current inactivation has been shown to underly the Timothy syndrome, a monogenetic "model disease" for ASD (Splawski et al. 2004; Breitenkamp et al. 2015). (3) In our previous studies, we identified functional effects of $Ca_V\beta_2$ variants when co-expressed with $Ca_V1.2$ (Breitenkamp et al. 2014; Despang et al. 2020; Graziano et al. 2021). For the following reasons, $Ca_V2.2$ was chosen as a second VGCC pore subunit for our analysis of the $Ca_V\beta_{1b\_R296C}$ variant: $Ca_V2.2$ is expressed predominantly in neurons where most of the central nervous system's synapses rely on $Ca_V2.2$ and $Ca_V2.1$ for fast synaptic transmission (Wheeler et al. 1994; Catterall et al. 2021). Three different $Ca_V\beta$ subunits associate with the pore-forming subunit $Ca_V2.2$, of which $Ca_V\beta_{1b}$ is an isoform (Scott et al. 1996; Müller et al. 2010).

Material and methods

DNA constructs and site-directed mutagenesis

For functional analysis, the mutation p.R296C was introduced in human $Ca_V\beta_{1b}$ (NM_000723) by site-directed mutagenesis (Stratagene QuikChange Kit) and verified by sequencing. EGFP was used as reporter gene, which was co-expressed together with the $Ca_V\beta$-subunit by the bicistronic pIRES2-EGFP vector (Clontech). R296C forward primer 5'-cattgagcgctccaacacatgctccagcct-3'; R296C reverse primer 5'-aggctggagcatgtgttggagcgctcaatg-3'. For co-immunoprecipitation experiments, a hemagglutinin (HA) tag was introduced in the C-terminus of the respective $Ca_V\beta_{1b}$ isoform and a Flag tag was introduced at the N-terminus of Gem. Cloning was done by using an in-fusion cloning kit (Takara Bio Europe, Gothenburg, Sweden) according to the manufacturer's manual and verified by sequencing. EGFP was used as reporter gene for $Ca_V\beta_{1b}$ and YFP as reporter for Gem.

Cell culture and transfection

In brief, HEK-293 cells were grown in Petri dishes in Dulbecco's modified Eagle's medium (Gibco Thermo Fisher, Waltham, MA, USA) supplemented with 10% FCS (Biochrom GmbH, Berlin Germany). Cells were routinely passaged twice a week and incubated at 37°C under 5% CO_2 growth conditions. tsA-201 cells were cultured at 37°C and 5% CO_2 in a 60-mm-diameter cell culture dish in 4-ml DMEM GlutaMAX medium (Biochrom GmbH, Berlin Germany) with 10% FCS (Biochrom GmbH, Berlin Germany) and penicillin-streptomycin (Sigma-Aldrich, St. Louis, MO, USA). Cells were routinely passaged twice a week. HEK-293 and tsA-201 cells were transfected using standard calcium phosphate method (Koch et al. 2016). For whole-cell and single-channel recordings, HEK-293 cells were transfected with a 1:0.5:1.5 ratio of $Ca_V1.2$ (α1c#77, NM_001129843.2) or $Ca_V2.2$ (NM_000718.3), either human WT (NM_000723) or mutant $Ca_V\beta$-subunit and human $Ca_V\alpha_2$-δ_1-subunit (NM_000722.3). For co-immunoprecipitation experiments, tsA-201 cells were transfected with a 1:2 ratio of either human WT or mutant $Ca_V\beta_{1b}$_HA-subunit and human Flag-Gem.

Co-immunoprecipitation and Western blot

The Gem and $Ca_V\beta$ co-immunoprecipitation experiments were performed as described previously (Despang et al. 2020). In brief, tsA cells were harvested 48–72 h after transfection in ice cold PBS and lysed in lysis buffer (50-mM Tris; 100-mM NaCl; 10-mM EDTA; 0.4% TritonX-100; 0.4% NP-40; pH: 7.5 with HCl). Protease inhibitor cocktail tablets (Sigma-Aldrich) were added immediately before lysing cells. Cell lysates were incubated for 1h at 4°C with rotation and afterwards for 30 min on ice. Cell lysates were then centrifuged for 15 min to remove cell debris. Lysate of 400µl of was incubated with 50µl (500µg)-Pierce™ Protein A/G Magnetic Beads (Thermo Scientific) and 5µl-anti-FLAG-Antibody M2 (Sigma-Aldrich) or 10-µl anti-HA 3F10 (Roche) at 4°C overnight. Beads were washed two times for 15–30 min in lysis buffer, and then proteins were eluted in 2x Laemmli buffer, incubated at 50°C for 10 min and frozen at −20°C. Elutions were separated using SDS-PAGE, followed by immunoblotting with anti-HA antibody (1:1000, Covance) and anti-FLAG antibody M2 (1:1000, Sigma-Aldrich).

Electrophysiological recordings

Whole-cell recordings were performed as in our previous studies (Breitenkamp et al. 2014; Despang et al. 2020; Graziano et al. 2021). Recordings of EGFP-positive cells were obtained 48–72 h after transfection. Immediately prior to recording, cells kept in 35-mm culture dishes were washed at room temperature (19–23°C) with bath solution. For whole-cell experiments with $Ca_V\beta_{1b}$ and α1C ($Ca_V1.2$), the bath solution contained (in mM) 10 $BaCl_2$, 1 $MgCl_2$, 10 HEPES, 65 CsCl, 40 TEA-Cl, 10 Glucose (pH 7.3 with TEA-OH), and the pipette solution (in mM) 140 CsCl, 10 EGTA, 9 HEPES, 1 $MgCl_2$, and 4 MgATP (pH 7.3 with CsOH). For whole-cell experiments with $Ca_V\beta_{1b}$ and α1B ($Ca_V2.2$), the bath solution contained (in mM) 20 $BaCl_2$, 1 $MgCl_2$, 10 HEPES, 125 NaCl (pH 7.3 with NaOH), and pipette solution (in mM) 135 CsCl, 10 EGTA, 10 HEPES, and 4 MgATP (pH 7.5 with CsOH). Holding potential was −80 mV. Patch pipettes made from borosilicate glass (1.7-mm diameter and 0.283-mm wall thickness, Hilgenberg GmbH, Malsfeld, Germany) were pulled using a Sutter Instrument P-97 horizontal puller and fire-polished using a Narishige MF-83 microforge (Narishige Scientific Instrument Lab, Tokyo, Japan). Pipette resistance was 2–4 MΩ. Using a holding potential of −80 mV, currents were elicited by applying 500, 1000, or 1500 ms test pulses of −40 mV to +50 mV. Currents were sampled at 10 kHz and filtered at 2 kHz. We used the Clampex software pClamp 10 and an Axopatch 200B amplifier (Molecular Devices, Sunnyvale, CA, USA).

Voltage dependence of Ba^{2+} whole-cell current inactivation was determined with a two-pulse protocol (a 2500-ms prepulse followed by a 200-ms test pulse at +10mV). For steady-state inactivation, the relative magnitude of inward current elicited during the second pulse was plotted as a function of the voltage of the conditioning first pulse. Data were analyzed using pClamp10 (Molecular Devices, Sunnyvale, CA, USA) and GraphPad 6 Prism. Currents were filtered at 2 kHz. Data were fitted to a Boltzmann function to obtain the half point (V0.5) and slope factor (dV) for the voltage dependence of inactivation. Fits were performed after subtracting the offset from the peak values of the steady-state inactivation data. Offset was defined as a deviation from zero at the end of a fully inactivating current (at the end of the test pulse at +10mV). For voltage dependence of activation, data were fitted by combined Ohm and Boltzmann relation $I(V) = (V–VR) \times \frac{G_{max}}{\left(1+\exp\frac{(V_{0.5}-V)}{dV}\right)}$ according to Karmazinova and Lacinova (Karmažínová and Lacinová 2010).

Single-channel recordings were performed at room temperature (19–23°C) using EGFP-positive cells 48–72 h after transfection. The bath solution contained (in mM) 120 K-glutamate, 25 KCl, 2 $MgCl_2$, 10 HEPES, 1 $CaCl_2$, 1 Na-ATP, and 2 EGTA (pH 7.4 with KOH). Patch pipettes were made from borosilicate glass (1.7-mm diameter and 0.283-mm wall thickness, Hilgenberg GmbH, Malsfeld, Germany) using a Narishige PP-83 vertical puller, Sylgard coated and fire-polished using a Narishige MF-83 microforge (Narishige Scientific Instrument Lab, Tokyo, Japan). Pipette resistance was 5–7 MΩ. Pipettes were filled using an internal solution containing (in mM) 110 $BaCl_2$ and 10 HEPES (pH 7.3 with TEA-OH). Single calcium channels were recorded in the cell-attached configuration (depolarizing test pulses of 150 ms at 1.67 Hz from −20mV to +20 mV in 10 mV steps from a holding potential of −100mV). An Axopatch 1D amplifier with pClamp 5.5 software (both from Axon Instruments, Foster City, CA, USA) was used for pulse generation, data acquisition (10 kHz), and filtering (2 kHz, −3 dB, 4-pole Bessel). Experiments were analyzed when channel activity persisted > 180 sweeps using pClamp 10 software (Molecular Devices).

Data analysis

Most experimental data are shown as raw currents, i.e., without capacity or leak subtraction. In a few experiments, for reasons of clarity, the capacitive transients were removed off-line. For calculation of the activation, the leak-current component was obtained from hyperpolarizing voltage steps from V_h and fitted using linear regression. The extrapolated leak current was then subtracted from the current-voltage (I-V) plot before estimation of the reversal potential. For

single-channel analysis, leak and capacity currents were digitally subtracted using pClamp 10 software (Molecular Devices). Channel openings and closures were determined using the half-height criterion. The availability (fraction of active sweeps, F_{active}), open probability (P_{open}), and mean open time were analyzed for single-channel as well as multi-channel patches. For the latter, these parameters were corrected for the number of channels in the patch (Herzig et al. 2007).

Statistical analysis

Electrophysiological data were obtained in experiments revealed from ≥ 3 individual transfections per plasmid composition and are shown as mean ± SEM. Experiments with WT and mutant were performed on the same day. Data were analyzed using unpaired two-sided Student *t* tests. Differences were considered statistically significant if $p < 0.05$.

Ethics approval

The local ethics committee approved the analyses (ref. No. 04-223) as described earlier (Breitenkamp et al. 2014).

Results

Description and genetic assessment of the $Ca_V\beta_{1b}$ mutation

We refer to the same probes analyzed previously (Breitenkamp et al. 2014). In a mutation screening involving 155 ASD patients, we found a rare missense mutation in the candidate gene *CACNB1* leading to an arginine-to-cysteine exchange (p.R296C) in the highly conserved GK-domain of the $Ca_V\beta_1$ subunit (NP_000714.3). The variant was found in a male patient (AGRE ID: AU09935301), but in none of 259 matching controls. The mutation was present in all splice variants of the patient's *CACNB1* gene. No other pathogenic or suspicious mutations known to contribute to neurodevelopmental disorders were found. No data on the presence of the *CACNB1* mutation in his parents are available, but they were not diagnosed with ASD.

The variant (chr17:37340296G>A; GRCh37) is listed in dbSNP (rs746198242) and in the gnomAD and ExAC databases with an allele frequency of 1.6×10^{-5} and 1.7×10^{-5}, respectively. The here presented *CACNB1* variant p.R296C is not listed in ClinVar (https://www.ncbi.nlm.nih.gov/clinvar) and has not been linked to ASD so far. According to the web-based program "PolyPhen2" (Adzhubei et al. 2010), the p.R296C missense variant is classified as damaging with 100% probability. According to standards and guidelines for the international interpretation of sequence variants (Richards et al. 2015), the rare frequency, the location of the variant in an essential and highly conserved protein domain, and the predictions render this variant a "variant of uncertain significance" (class 3, due to AGMC criteria PM2, PM1 and PP3). In the following, we tested for putative functional effects in electrophysiological patch-clamp experiments. Unlike $Ca_V\beta_{1a}$ and $Ca_V\beta_{1c}$, the splice variant $Ca_V\beta_{1b}$ is expressed in the brain and is upregulated during ontogenesis (Buraei and Yang 2010). Therefore, we subcloned the mutation into the splice form $Ca_V\beta_{1b}$ (NM_000723).

Functional characterization of the $Ca_V\beta_{1b}$ variant

Whole-cell recordings

When co-expressing $Ca_V1.2$ with the $Ca_V\beta_{1b\_R296C}$ mutant, whole-cell current density was decreased compared to the wild-type $Ca_V\beta_{1b}$ (e.g., 21.0 ± 2.5 vs. 11.7 ± 1.6 pA/pF at 0 mV, p=0.003; Figs. 1a and b) along with a shift in the half-maximal activation potential $V0.5_{act}$ to more positive values (−13.3 ± 1.9 vs. −8.0 ± 1.5 mV, p=0.038; Fig. 1c). Furthermore, time-dependent inactivation was increased at 150 ms (e.g., 25 ± 4 vs. 39 ± 4 % at +10 mV, p=0.015) and 300 ms (e.g. 52 ± 4 vs. 65 ± 4 % at +10 mV, p=0.03) (Figs. 2a and b). No statistically significant differences were found at 500 ms, 1000 ms, and 1500 ms (not shown). Analysis of steady-state inactivation revealed a non-significant (p=0.071) shift of $Ca_V\beta_{1b\_R296C}$ to more positive potentials compared to $Ca_V\beta_{1b\_WT}$ (Fig. 2c). Similar to $Ca_V1.2$, the current density was decreased when $Ca_V2.2$ was co-expressed with $Ca_V\beta_{1b\_R296C}$ compared to $Ca_V\beta_{1b\_WT}$, although the difference was only statistically significant at 0 mV (p=0.045). $V0.5_{act}$ was shifted to more positive values by $Ca_V\beta_{1b\_R296C}$ (−1.1 ± 2.4 vs. 6.2 ± 1.6 mV, p=0.017; Fig. 3c). No difference in time-dependent inactivation or steady-state inactivation was found between mutant and wild-type $Ca_V\beta_{1b}$ subunits (not shown).

Single-channel recordings

At the single-channel level, $Ca_V\beta_{1b\_R296C}$ showed statistically significant inhibitory effects on both $Ca_V1.2$ and $Ca_V2.2$. Fraction of active sweeps (F_{active}) and open probability (P_{open}) of $Ca_V1.2$ were significantly reduced when co-expressing $Ca_V\beta_{1b\_R296C}$ instead of the $Ca_V\beta_{1b\_WT}$ (Figs. 4 ba and bb). The latency until a first opening and the extent of inactivation were increased (Figs. 4 bc and bd). Similar effects of $Ca_V\beta_{1b\_R296C}$ were seen on the activity of single $Ca_V2.2$ reaching statistical significance for fraction of active sweeps and first latency (Figs. 4 ca and cc).

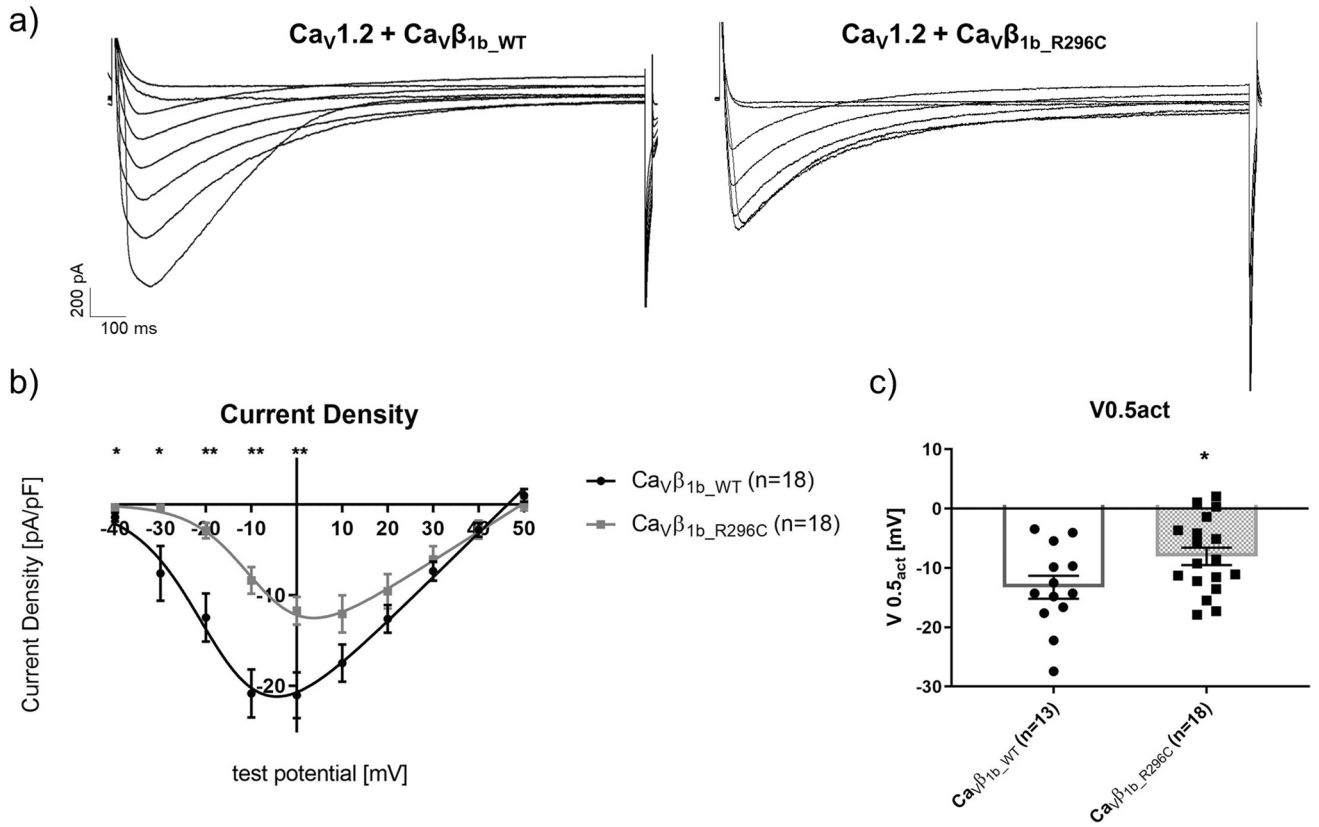

Fig. 1 Whole-cell currents mediated by $Ca_V1.2$ co-expressed with $Ca_V\alpha_2$-δ_1 and either the wild-type ($Ca_V\beta_{1b\_WT}$) or mutant ($Ca_V\beta_{1b\_R296C}$) form of $Ca_V\beta_{1b}$. (**a**) Exemplary traces of whole-cell recordings with either $Ca_V\beta_{1b\_WT}$ (left) or $Ca_V\beta_{1b\_R296C}$ (right). (**b**) IV-relationships of $Ca_V\beta_{1b\_WT}$ (n=18) and $Ca_V\beta_{1b\_R296C}$ (n=18). Starting from a holding potential of −80 mV, currents were elicited at test potentials from −40 to +50 mV in 10 mV increments using 10 mM Ba^{2+} as charge carrier. (**c**) Test potential of the half-maximal activation ($V0.5_{act}$). Data were obtained using patch-clamp recordings in the whole-cell configuration. *,**: $p<0.05$ and $p<0.01$ in Student's t tests

Effects of Gem co-expression on whole-cell and single-channel activity

Gem is an RGK-protein that interacts with auxiliary $Ca_V\beta$ subunits and inhibits VGCCs (Yang and Colecraft 2013). As in our previous study (Despang et al. 2020), we analyzed the interaction of Gem with the mutated $Ca_V\beta_{1b}$ and the effects on $Ca_V1.2$-mediated Ba^{2+} currents. Similar to our previous findings with $Ca_V\beta_{2d}$, co-immunoprecipitation experiments showed an interaction of Gem with both mutated and wild-type $Ca_V\beta_{1b}$ subunits (Fig. 5a). In whole-cell experiments, we saw an almost complete inhibition of Ba^{2+} currents compared to experiments without Gem transfection (Figs. 5b and c). Gem reduced whole-cell currents similarly in the presence of $Ca_V\beta_{1b\_WT}$ or $Ca_V\beta_{1b\_R296C}$ (Fig. 5c). Corresponding to our findings at the whole-cell level, we found Gem to reduce single-channel activity, e.g., by lowering the fraction of active sweeps or open probability (Fig. 6).

Discussion

In the last years, the evidence for the involvement of VGCCs in ASD has been growing and actually for most VGCC genes evidence for an association with ASD was found (Breitenkamp et al. 2015). Our group focuses on auxiliary $Ca_V\beta$ subunits of VGCCs and their putative contribution to this complex-genetic disease. To our knowledge, this is the first report of a mutation in *CACNB1* identified in an ASD patient. We previously described different mutations of the $Ca_V\beta_2$ isoform which led to an increase of $Ca_V1.2$ activity both at the single-channel and the whole-cell level (Breitenkamp et al. 2014; Despang et al. 2020). In a more recent study, we could show that another mutation in *CACNB2* led to a reduced inactivation of whole-cell currents, which also indicates increased $Ca_V1.2$ activity (Graziano et al. 2021). Taken together, the increase in $Ca_V1.2$ activity appears to be a common feature

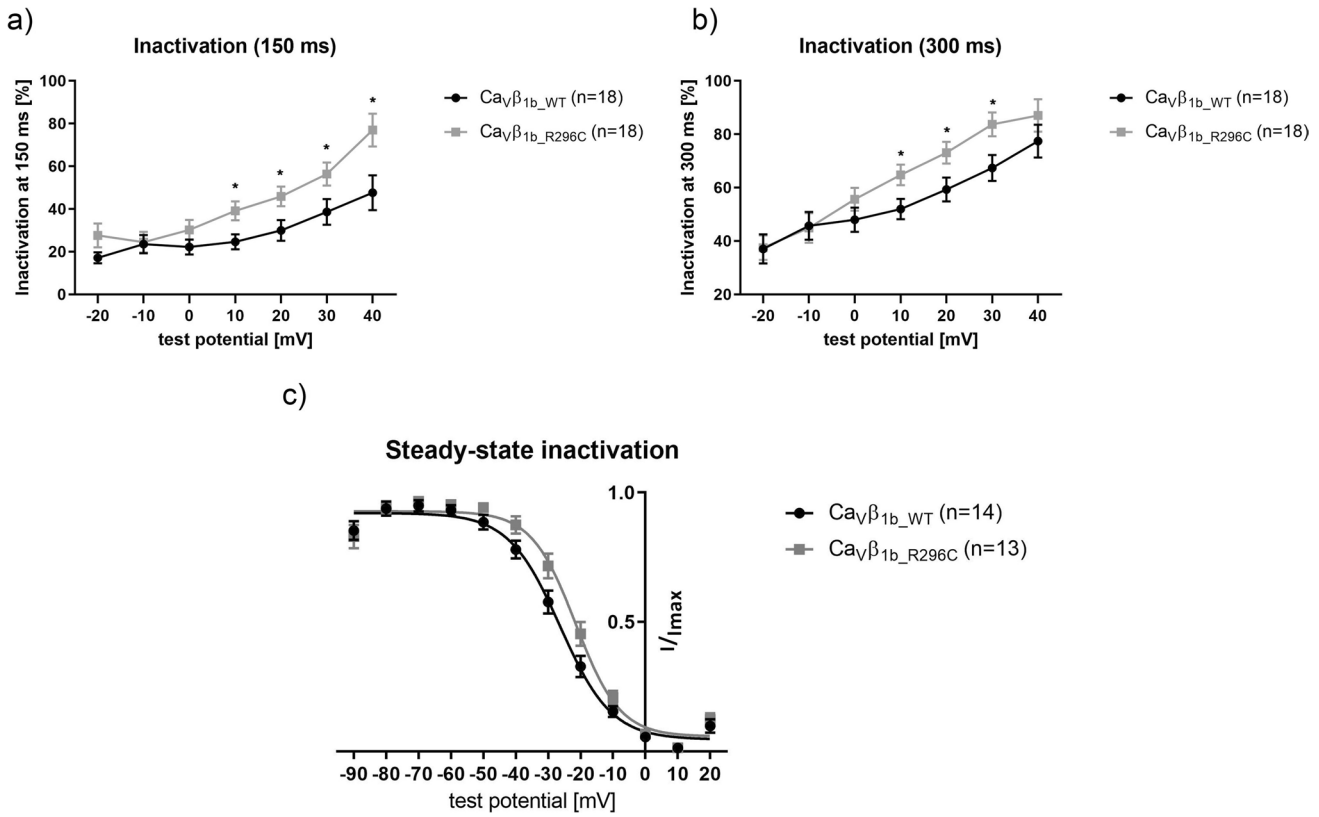

Fig. 2 Time-dependent inactivation behavior of $Ca_V1.2$ co-expressed with $Ca_V\alpha_2$-δ_1 and either the wild-type ($Ca_V\beta_{1b\_WT}$; n=18) or mutant ($Ca_V\beta_{1b\_R296C}$; n=18) form of $Ca_V\beta_{1b}$, analyzed as the fraction of peak current inactivated after 150 ms (**a**) or 300 ms (**b**) of depolarization. (**c**) Voltage-dependent steady-state inactivation behavior of $Ca_V\beta_{1b\_WT}$ (n=14) compared to $Ca_V\beta_{1b\_R296C}$ (n=13). Data were obtained using patch-clamp recordings in the whole-cell configuration. *: $p<0.05$ in Student's t tests

among $Ca_V\beta_2$ variants found in ASD patients. In contrast, the *CACNB1* mutation described here results in a $Ca_V\beta_1$ variant that, compared to a wild-type $Ca_V\beta_1$, decreases current density and shifts half-maximal activation to more positive potentials when co-expressed with $Ca_V1.2$ or $Ca_V2.2$ and it increases inactivation of $Ca_V1.2$. These findings are consistent with the reduced single-channel activity of both, L-type ($Ca_V1.2$) and N-type ($Ca_V2.2$) VGCCs. $Ca_V\beta_{1b\_R296C}$ thus can be considered a loss-of-function mutation.

To our knowledge, reduced single-channel activity has not been described in the context of ASD-associated VGCC variants so far. Even more, the only (electrophysiological) loss-of-function variant of $Ca_V\beta_1$ we are aware of was described in the context of Brugada syndrome, a cardiac disease associated with arrhythmia (Antzelevitch et al. 2007). Interestingly, there are $Ca_V\beta_2$ variants associated with Brugada syndrome that lead to decreased whole-cell currents ($Ca_V\beta_{2b\_S481L}$) or accelerated inactivation of $Ca_V1.2$ ($Ca_V\beta_{2b\_T11I}$) (Antzelevitch et al. 2007; Cordeiro et al. 2009). The affected $Ca_V\beta_{2b}$ subunit is the most abundant $Ca_V\beta$ subunit in the heart but is also expressed in the brain (Hullin et al. 2007; Buraei and Yang 2010). Nevertheless, the patients described in the context of Brugada syndrome did not show a neurodevelopmental phenotype. Like $Ca_V\beta_{2b}$, $Ca_V\beta_{1b}$ is one of several $Ca_V\beta$ subunits expressed in the brain (in addition to, e.g., $Ca_V\beta_{2a,e}$, $Ca_V\beta_3$, and $Ca_V\beta_4$) (Buraei and Yang 2010). Similar to $Ca_V\beta_2$ variants found in ASD patients (Despang et al. 2020), the $Ca_V\beta_{1b}$ variant described here shows a heterozygous expression profile. It has been shown that different $Ca_V\beta$ isoforms can compete for the interaction with the $Ca_V1.2$ subunit by this modulating VGCC activity dynamically on a minute timescale (Jangsangthong et al. 2011). In another study, co-expression of $Ca_V\beta_{2a}$ and $Ca_V\beta_3$ resulted in two biophysical distinct channel populations (Jones et al. 1998). Thus, we cannot exclude that the inhibitory effects of the $Ca_V\beta_{1b\_R296C}$ variant observed in the current study might be (partially) compensated by other $Ca_V\beta$ isoforms and/or splice variants in a more physiological expression system.

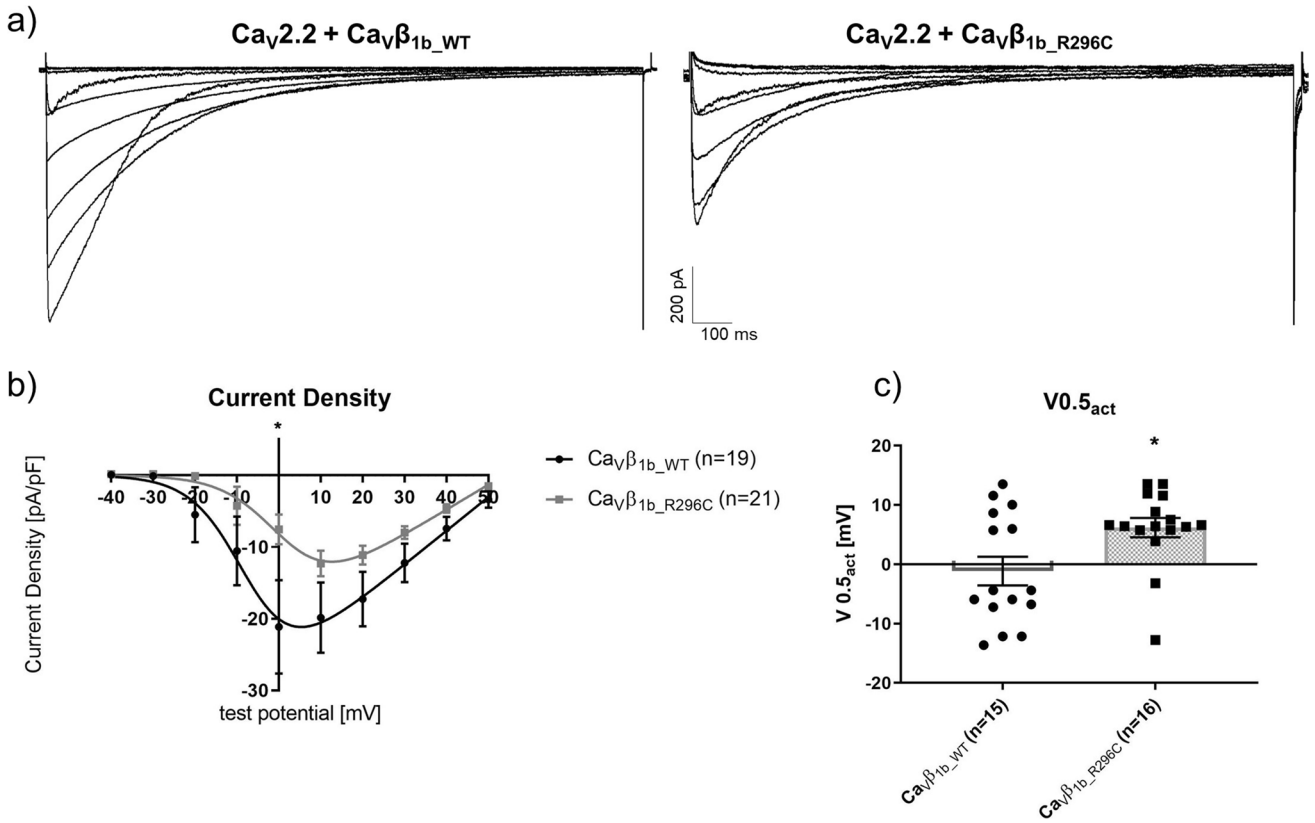

Fig. 3 Whole-cell currents mediated by $Ca_V2.2$ co-expressed with $Ca_V\alpha_2$-δ_1 and either the wildtype ($Ca_V\beta_{1b\_WT}$) or mutant ($Ca_V\beta_{1b\_R296C}$) form of $Ca_V\beta_{1b}$. (**a**) Exemplary traces of whole-cell recordings with either $Ca_V\beta_{1b\_WT}$ (left) or $Ca_V\beta_{1b\_R296C}$ (right). (**b**) IV-relationships of $Ca_V\beta_{1b\_WT}$ (n=19) and $Ca_V\beta_{1b\_R296C}$ (n=21). Starting from a holding potential of -80 mV, currents were elicited at test potentials from -40 to +50 mV in 10 mV increments using 20 mM Ba^{2+} as charge carrier. **(c)** Test potential of the half-maximal activation ($V0.5_{act}$). Data were obtained using patch-clamp recordings in the whole-cell configuration. *: $p<0.05$ in Student's *t* tests

The mutation described in this study lies within the GK-domain of $Ca_V\beta_1$, a region well established as a protein-protein interaction site, especially for the intramolecular interactions with the SH3-domain critically involved in the function of $Ca_V\beta$ subunits (Buraei and Yang 2010). Alterations affecting these domains have been shown to change the effects of $Ca_V\beta$ subunits on VGCC gating (Chen et al. 2009). Furthermore, GK-GK domain or SH3-SH3 domain interactions are involved in $Ca_V\beta$ dimerization (Lao et al. 2010; Miranda-Laferte et al. 2011). Of note, the formation of SH3-SH3 dimers is probably mediated by a cysteine residue (Miranda-Laferte et al. 2011). Whether the introduction of a cysteine in the GK-domain of our $Ca_V\beta_{1b\_R296C}$ variant has a similar effect should be investigated in future studies. According to the web-based prediction program DiANNA 1.1 (Ferrè and Clote 2005), the exchange from arginine to cysteine results in an additional disulfide bond and by this a potentially misfolded tertiary structure of the mutant compared to the wild-type $Ca_V\beta_{1b}$.

It has been shown that the $Ca_V\beta_{1b}$ subunit prevents $Ca_V1.2$ from degradation and facilitates its export from the endoplasmic reticulum (Altier et al. 2011). Similarly, it prevented $Ca_V2.2$ from proteasomal degradation (Page et al. 2016). In this context, a recent study could show that the $Ca_V\beta$ subunit is imperative for the anterograde transport of $Ca_V1.2$ channels to the plasma membrane, while the retrograde transport seems to be $Ca_V\beta$ independent (Conrad et al. 2021). Thus, we cannot exclude that beneath single-channel activity, VGCC expression might be affected by the examined $Ca_V\beta$ variant. RGK-proteins in general are known VGCC inhibitors by directly inhibiting the activity of VGCCs or altering number of channels at the membrane (Buraei et al. 2015). While some of the RKG-proteins can regulate VGCC activity by directly interacting with the pore-forming subunit of VGCC complexes, Gem utilizes a solely $Ca_V\beta$-dependent mode of action (Puckerin et al. 2016, 2018). In the present study, co-expression of the RGK-protein Gem similarly reduced whole-cell currents

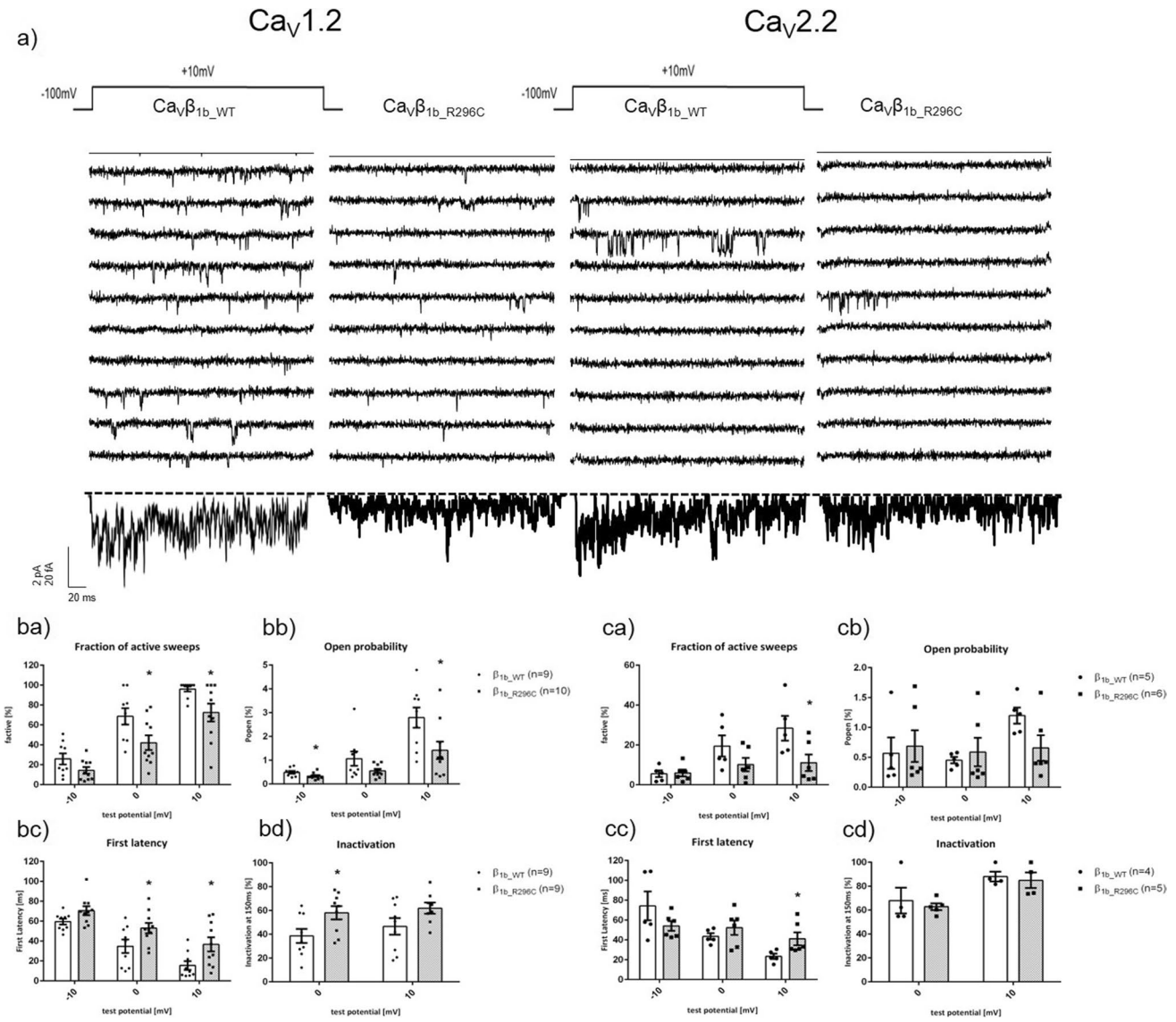

Fig. 4 Gating of single L-type ($Ca_V1.2$, left) and N-type ($Ca_V2.2$, right) channels in the presence of a wildtype ($Ca_V\beta_{1b\_WT}$) or the mutant ($Ca_V\beta_{1b\_R296C}$) form of $Ca_V\beta_{1b}$. (**a**) Exemplary traces. Top: pulse protocol (150 ms duration, holding potential of -100 mV, test pulse to +10 mV). Middle: ten consecutive traces for each channel complex. Bottom: ensemble average currents of the respective experiments. (**b, c**) Single-channel gating parameters of human $Ca_V1.2$ (**ba-bd**; n=9–10) or $Ca_V2.2$ (**ca-cd**; n=5–6) transiently expressed in HEK-293 cells and co-transfected with $Ca_V\beta_{1b\_WT}$ or $Ca_V\beta_{1b\_R296C}$ and a human $Ca_V\alpha_2$-δ_1. Statistical analyses revealed a significant decrease in the fraction of active sweeps and an increase in first latency in the presence of $Ca_V\beta_{1b\_R296C}$ (**ba, bc, ca, cc**). The reduction of the open probability was statistically significant with $Ca_V1.2$ (**bb**) but slightly missed statistical significance with $Ca_V2.2$ (**cb**; p=0.07). Inactivation was significantly increased when co-expressing $Ca_V\beta_{1b\_R296C}$ together with $Ca_V1.2$ (**bd**), but unaffected with $Ca_V2.2$ (**cd**). Data were obtained using patch-clamp recordings in the cell-attached configuration using 110mM Ba^{2+} as charge carrier. *: p<0.05 in Student's t tests

mediated by VGCCs co-expressed with either $Ca_V\beta_{1b\_R296C}$ or $Ca_V\beta_{1b\_WT}$. In our previous study, $Ca_V\beta_2$ variants found in ASD patients showed a differential modulation of $Ca_V1.2$ compared to each other and to the respective wild-type $Ca_V\beta_2$ (Despang et al. 2020). Of note, this was also seen in differences between Gem-mediated inhibitory effects. RGK-proteins have been proposed to have potentials as therapeutic tools for a differential and specific modulation of VGCCs (Colecraft 2020). It is tempting to speculate that RGK proteins might be a tool to differentially compensate for changes of VGCC-mediated currents that are due to mutated $Ca_V\beta$ subunits.

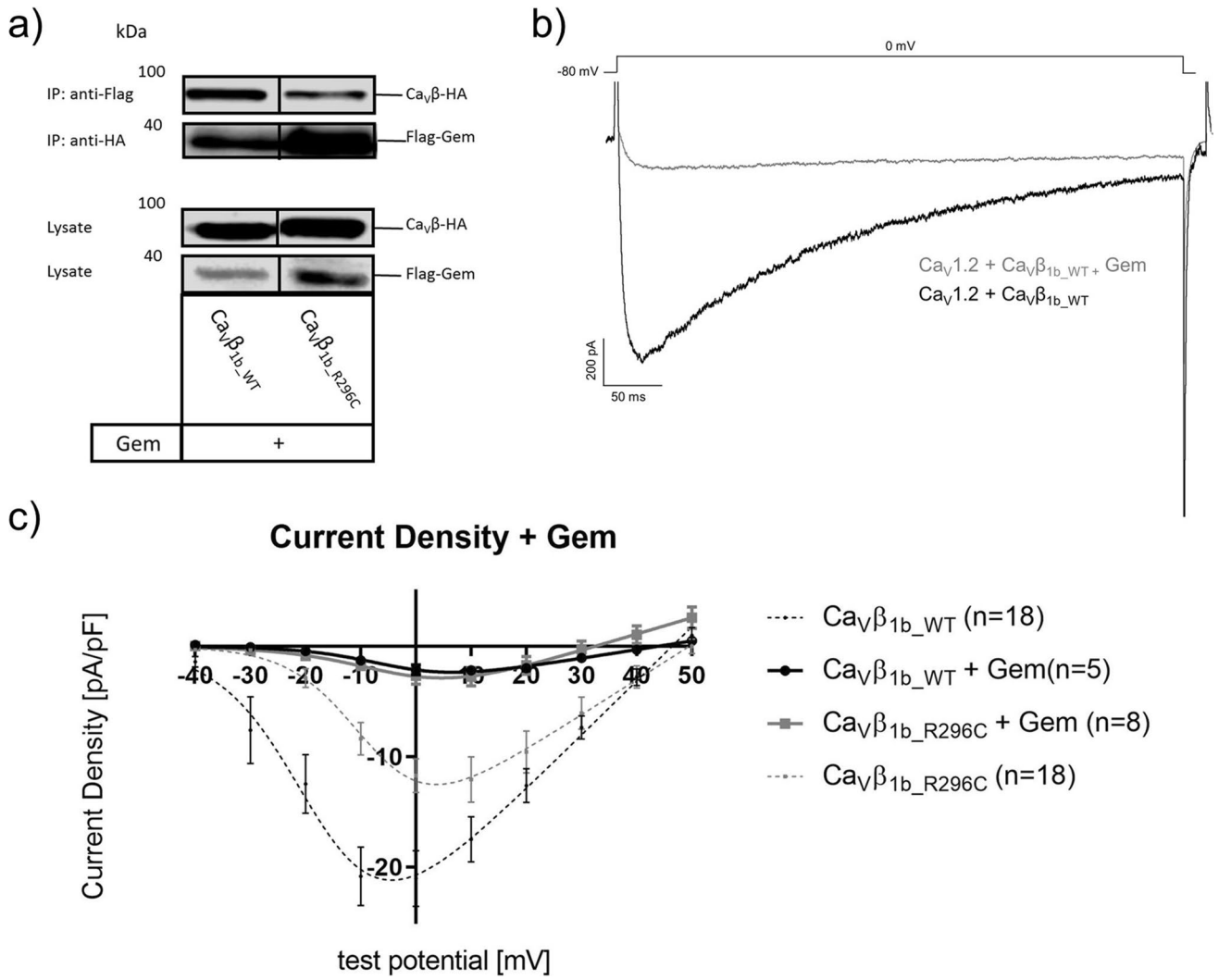

Fig. 5 $Ca_V\beta$-Gem interaction and Gem effects on $Ca_V1.2$-mediated whole-cell currents in the presence of either the wild-type ($Ca_V\beta_{1b\_WT}$) or mutant ($Ca_V\beta_{1b\_R296C}$) form of $Ca_V\beta_{1b}$. (**a**) Gem binds to both, $Ca_V\beta_{1b\_WT}$ and $Ca_V\beta_{1b\_R296C}$. For co-immunoprecipitation experiments, tsA-201 cells were co-transfected with cDNA of Flag-tagged Gem and HA-tagged $Ca_V\beta_{1b}$ subunits as indicated. Flag-tagged Gem proteins were immunoprecipitated (IP) and bound $Ca_V\beta_{1b}$ protein was detected by Western-blot. Interaction was confirmed by reciprocal immunoprecipitation. Cell lysates were blotted with a HA- or Flag-antibody to verify $Ca_V\beta_{1b}$ and Gem expression, respectively. All experiments were repeated at least three times. (**b**) Exemplary traces of whole-cell recordings in HEK293 cells with expression of $Ca_V\beta_{1b\_WT}$ at a test potential of 0 mV. Exemplary traces are shown as overlay to better visualize the reduction of currents in the presence of Gem. (**c**) IV-relationships in Gem-transfected HEK293 cells with expression of either $Ca_V\beta_{1b\_WT}$ or $Ca_V\beta_{1b\_R296C}$ (solid curves). For comparison, IV-relationships without co-transfection of Gem is shown as dashed curves (taken from Fig. 1). Starting from a holding potential of −80 mV, currents were elicited at test potentials from −40 to +50 mV in 10 mV increments using 10 mM Ba^{2+} as charge carrier. Data were obtained using patch-clamp recordings in the whole-cell configuration

The alterations caused by co-expressing the $Ca_V\beta_{1b\_R296C}$ variant appear to be less pronounced on $Ca_V2.2$ compared to $Ca_V1.2$, both in respect to whole-cell currents and single-channel gating. Differences between modulation of Ca_V1 and Ca_V2 VGCCs by $Ca_V\beta$ subunits have already been described (Buraei and Yang 2010). Future studies should address this in more detail.

Conclusion

While evidence for *CACNB2* involvement in ASD is growing, this is the first report of a *CACNB1* variant found in an ASD patient that shows functional consequences, at least at the molecular level. Interestingly, the effects of the $Ca_V\beta_{1b\_R296C}$ described here are opposite to those described for $Ca_V\beta_2$ variants previously, i.e. an inhibitory

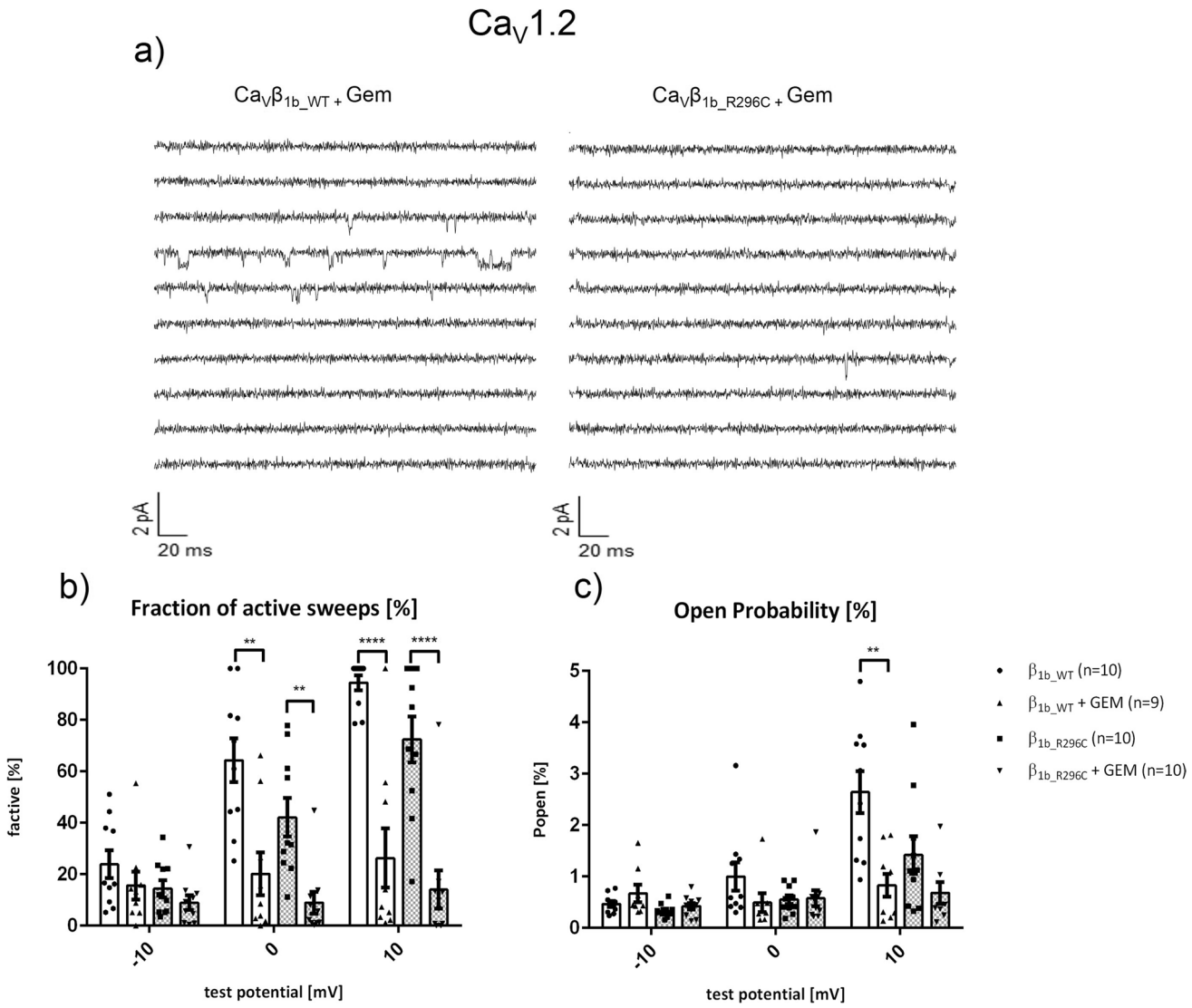

Fig. 6 Effects of Gem on single-channel behavior of L-type ($Ca_V1.2$) calcium channels in the presence of either the wild-type ($Ca_V\beta_{1b\_WT}$) or the mutant ($Ca_V\beta_{1b\_R296C}$) form of $Ca_V\beta_{1b}$. (**a**) Ten representative consecutive traces obtained at a test potential of +10 mV in Gem-transfected HEK293 cells expressing either $Ca_V\beta_{1b\_WT}$ (left) or $Ca_V\beta_{1b\_R296C}$ (right). Fraction of active sweeps (**b**) and open probability (**c**) indicate similarly reduced activity of single $Ca_V1.2$ when Gem was co-expressed together with either $Ca_V\beta_{1b\_WT}$ or $Ca_V\beta_{1b\_R296C}$. Number of experiments are indicated in the figure. Asterisks indicate $p<0.05$ in Student's *t* tests. Data were obtained using patch-clamp recordings in the cell-attached configuration (charge carrier: 110 mM Ba^{2+})

instead of a stimulatory effect compared to the respective WT $Ca_V\beta$ isoform. This might indicate differential roles of different $Ca_V\beta$ isoforms in the context of ASD. However, the electrophysiological effects we have described at the molecular and cellular level need further investigation in models of more pathophysiological relevance.

Supplementary Information The online version contains supplementary material available at https://doi.org/10.1007/s00210-022-02213-7.

Acknowledgement We thank Marion Brill, Cora Fried and Sigrid Kirchmann-Hecht for their excellent technical support.

Availability of data and material Upon request.

Code availability Not applicable.

Author contributions JM and PD conceived and designed the research. PD and AB conducted the experiments. PD, AB, SS, and EK analyzed the data. PD and JM wrote the manuscript. All authors read and approved the manuscript. All data were generated in-house, and the authors state that no paper mill was used.

Funding Open Access funding enabled and organized by Projekt DEAL. Supported by the Koeln Fortune Program/Faculty of Medicine, University of Cologne (Project No. 349/2020 to PD). Supported by the rectorate of the University of Cologne (PLAN to JM).

Declarations

Ethics approval Positive vote of the local ethics committee (04-223).

Consent to participate Not applicable.

Consent for publication All authors approved the manuscript to be published.

Competing interests The authors declare no competing interests.

References

Adzhubei IA, Schmidt S, Peshkin L et al (2010) A method and server for predicting damaging missense mutations. Nat. Methods 7:248–249

Altier C, Garcia-Caballero A, Simms B et al (2011) The Cavβ subunit prevents RFP2-mediated ubiquitination and proteasomal degradation of L-type channels. Nat Neurosci 14:173–182. https://doi.org/10.1038/nn.2712

Antzelevitch C, Pollevick GD, Cordeiro JM et al (2007) Loss-of-function mutations in the cardiac calcium channel underlie a new clinical entity characterized by ST-segment elevation, short QT intervals, and sudden cardiac death. Circulation 115:442–449. https://doi.org/10.1161/CIRCULATIONAHA.106.668392

Breitenkamp AF, Matthes J, Herzig S (2015) Voltage-gated Calcium Channels and Autism Spectrum Disorders. Curr Mol Pharmacol 8:123–132

Breitenkamp AFS, Matthes J, Nass RD et al (2014) Rare Mutations of CACNB2 Found in Autism Spectrum Disease-Affected Families Alter Calcium Channel Function. PLoS One 9:e95579. https://doi.org/10.1371/journal.pone.0095579

Buraei Z, Lumen E, Kaur S, Yang J (2015) RGK regulation of voltage-gated calcium channels. Sci China Life Sci 58:28–38. https://doi.org/10.1007/s11427-014-4788-x

Buraei Z, Yang J (2010) The β subunit of voltage-gated Ca2+ channels. Physiol Rev 90:1461–1506. https://doi.org/10.1152/physrev.00057.2009

Campiglio M, Flucher BE (2015) The Role of Auxiliary Subunits for the Functional Diversity of Voltage-Gated Calcium Channels. J Cell Physiol 230:2019–2031. https://doi.org/10.1002/jcp.24998

Cantor RM, Kono N, Duvall JA et al (2005) Replication of autism linkage: Fine-mapping peak at 17q21. Am J Hum Genet 76:1050–1056. https://doi.org/10.1086/430278

Catterall WA, Perez-Reyes E, Snutch TP, Striessnig J (2021) Voltage-gated calcium channels in GtoPdb v.2021.2. IUPHAR/BPS Guid to Pharmacol CITE 2021:. doi: 10.2218/gtopdb/F80/2021.2

Hang CY, Ling HL, Buchanan DR et al (2009) Functional dissection of the intramolecular Src homology 3-guanylate kinase domain coupling in voltage-gated Ca2+ channel β-subunits. FEBS Lett 583:1969–1975. https://doi.org/10.1016/j.febslet.2009.05.001

Colecraft HM (2020) Designer genetically encoded voltage-dependent calcium channel inhibitors inspired by RGK GTPases. J Physiol 598:1683–1693. https://doi.org/10.1113/JP276544

Conrad R, Kortzak D, Guzman GA et al (2021) CaVβ controls the endocytic turnover of CaV1.2 L-type calcium channel. Traffic 22:180–193. https://doi.org/10.1111/tra.12788

Cordeiro JM, Marieb M, Pfeiffer R et al (2009) Accelerated inactivation of the L-type calcium current due to a mutation in CACNB2b underlies Brugada syndrome. J Mol Cell Cardiol 46:695–703. https://doi.org/10.1016/J.YJMCC.2009.01.014

Despang P, Salamon S, Breitenkamp AF, et al (2020) Autism-associated mutations in the CaVβ2 calcium-channel subunit increase Ba2+-currents and lead to differential modulation by the RGK-protein Gem. Neurobiol Dis 136:. doi: 10.1016/j.nbd.2019.104721

Dolphin AC (2012) Calcium channel auxiliary α 2 δ and β subunits: Trafficking and one step beyond. Nat. Rev. Neurosci. 13:542–555

Ebert DH, Greenberg ME (2013) Activity-dependent neuronal signalling and autism spectrum disorder. Nature 493:327–337

Ferrè F, Clote P (2005) DiANNA: A web server for disulfide connectivity prediction. Nucleic Acids Res 33. https://doi.org/10.1093/nar/gki412

Graziano C, Despang P, Palombo F et al (2021) A New Homozygous CACNB2 Mutation has Functional Relevance and Supports a Role for Calcium Channels in Autism Spectrum Disorder. J. Autism Dev. Disord. 51:377–381

Herzig S, Khan IFY, Gründemann D et al (2007) Mechanism of Ca v 1.2 channel modulation by the amino terminus of cardiac β 2 -subunits. FASEB J 21:1527–1538. https://doi.org/10.1096/fj.06-7377com

Hibino H, Pironkova R, Onwumere O et al (2003) Direct interaction with a nuclear protein and regulation of gene silencing by a variant of the Ca2+-channel β4 subunit. Proc Natl Acad Sci U S A 100:307–312. https://doi.org/10.1073/pnas.0136791100

Hofmann F, Flockerzi V, Kahl S, Wegener JW (2014) L-type CaV1.2 calcium channels: From in vitro findings to in vivo function. Physiol Rev 94:303–326. https://doi.org/10.1152/physrev.00016.2013

Hullin R, Matthes J, von Vietinghoff S, et al (2007) Increased expression of the auxiliary β<inf>2</inf>-subunit of ventricular L-type Ca^{2+} channels leads to single-channel activity characteristic of the heart failure. PLoS One 2:. doi: 10.1371/journal.pone.0000292

Jangsangthong W, Kuzmenkina E, Böhnke AK, Herzig S (2011) Single-channel monitoring of reversible L-type Ca 2+ channel Ca Vα 1-Ca Vβ subunit interaction. Biophys J 101:2661–2670. https://doi.org/10.1016/j.bpj.2011.09.063

Jones LP, Wei S, Yue DT (1998) Mechanism of Auxiliary Subunit Modulation of Neuronal α1E Calcium Channels. J Gen Physiol 112:125–143. https://doi.org/10.1085/jgp.112.2.125

Karmažínová M, Lacinová L (2010) Measurement of cellular excitability by whole cell patch clamp technique. Physiol Res 59:1–7

Koch P, Herzig S, Matthes J (2016) An expert protocol for immunofluorescent detection of calcium channels in tsA-201 cells. J Pharmacol Toxicol Methods 82:20–25. https://doi.org/10.1016/j.vascn.2016.07.001

Lao QZ, Kobrinsky E, Liu Z, Soldatov NM (2010) Oligomerization of Cavbeta subunits is an essential correlate of Ca2+ channel activity. FASEB J 24:5013–5023. https://doi.org/10.1096/fj.10-165381

Meir A, Bell DC, Stephens GJ et al (2000) Calcium channel β subunit promotes voltage-dependent modulation of α1B by Gβγ. Biophys J 79:731–746. https://doi.org/10.1016/S0006-3495(00)76331-4

Miles JH (2011) Autism spectrum disorders-A genetics review. Genet. Med. 13:278–294

Miranda-Laferte E, Gonzalez-Gutierrez G, Schmidt S et al (2011) Homodimerization of the Src homology 3 domain of the calcium channel β-subunit drives dynamin-dependent endocytosis. J Biol Chem 286:22203–22210. https://doi.org/10.1074/jbc.M110.201871

Müller CS, Haupt A, Bildl W et al (2010) Quantitative proteomics of the Cav2 channel nanoenvironments in the mammalian brain. Proc Natl Acad Sci U S A 107:14950–14957. https://doi.org/10.1073/PNAS.1005940107/-/DCSUPPLEMENTAL/ST02.PDF

O'Roak BJ, Deriziotis P, Lee C et al (2011) Exome sequencing in sporadic autism spectrum disorders identifies severe de novo mutations. Nat Genet 43:585–589. https://doi.org/10.1038/ng.835

Page KM, Rothwell SW, Dolphin AC (2016) The CaVβ subunit protects the I-II loop of the voltage-gated calcium channel CaV2.2 from proteasomal degradation but not oligoubiquitination. J Biol Chem 291:20402–20416. https://doi.org/10.1074/jbc.M116.737270

Puckerin AA, Chang DD, Subramanyam P, Colecraft HM (2016) Similar molecular determinants on Rem mediate two distinct modes of inhibition of CaV1.2 channels. Channels 10:379–394. https://doi.org/10.1080/19336950.2016.1180489

Puckerin AA, Chang DD, Shuja Z, Choudhury P, Scholz J, Colecraft HM (2018) Engineering selectivity into RGK GTPase inhibition of voltage-dependent calcium channels. Proc Natl Acad Sci U S A 115:12051–12056. https://doi.org/10.1073/pnas.1811024115

Richards S, Aziz N, Bale S et al (2015) Standards and guidelines for the interpretation of sequence variants: A joint consensus recommendation of the American College of Medical Genetics and Genomics and the Association for Molecular Pathology. Genet Med 17:405–424. https://doi.org/10.1038/gim.2015.30

Scott VES, De Waard M, Liu H et al (1996) β Subunit Heterogeneity in N-type Ca2+ Channels. J Biol Chem 271:3207–3212. https://doi.org/10.1074/jbc.271.6.3207

Skafidas E, Testa R, Zantomio D et al (2014) Predicting the diagnosis of autism spectrum disorder using gene pathway analysis. Mol Psychiatry 19:504–510. https://doi.org/10.1038/mp.2012.126

Splawski I, Timothy KW, Sharpe LM et al (2004) CaV1.2 Calcium Channel Dysfunction Causes a Multisystem Disorder Including Arrhythmia and Autism. Cell 119:19–31. https://doi.org/10.1016/j.cell.2004.09.011

Trikalinos TA, Karvouni A, Zintzaras E et al (2006) A heterogeneity-based genome search meta-analysis for autism-spectrum disorders. Mol Psychiatry 11:29–36. https://doi.org/10.1038/sj.mp.4001750

Wheeler DB, Randall A, Tsien RW (1994) Roles of N-Type and Q-Type Ca 2+ Channels in Supporting Hippocampal Synaptic Transmission. Science (80-) 264:107–111. doi: https://doi.org/10.1126/science.7832825

Won H, Mah W, Kim E (2013) Autism spectrum disorder causes, mechanisms, and treatments: Focus on neuronal synapses. Front. Mol. Neurosci. 6

Yang T, Colecraft HM (2013) Biochimica et Biophysica Acta Regulation of voltage-dependent calcium channels by RGK proteins ☆. BBA - Biomembr 1828:1644–1654. https://doi.org/10.1016/j.bbamem.2012.10.005